AD_____
(Leave blank)

Award Number:
W81XWH-08-1-0380

TITLE:
Elucidating the Tumor Suppressive Role of SLITs in Maintaining the Basal Cell Niche

PRINCIPAL INVESTIGATOR:
Lindsay Hinck

CONTRACTING ORGANIZATION:
University of California, Santa Cruz
Santa Cruz, CA 95064

REPORT DATE:
July 2010

TYPE OF REPORT:
Annual

PREPARED FOR: U.S. Army Medical Research and Materiel Command
Fort Detrick, Maryland 21702-5012

DISTRIBUTION STATEMENT: (Check one)

√ Approved for public release; distribution unlimited

Distribution limited to U.S. Government agencies only; report contains proprietary information

REPORT DOCUMENTATION PAGE

Form Approved
OMB No. 0704-0188

1. REPORT DATE *(DD-MM-YYYY)*	**2. REPORT TYPE**	**3. DATES COVERED** *(From - To)*
07/31/10	Annual	1 JUL 2009 - 30 JUN 2010

4. TITLE AND SUBTITLE
Elucidating the Tumor Suppressive Role of SLITs in Maintaining the Basal Cell Niche

5a. CONTRACT NUMBER

5b. GRANT NUMBER
BC074170

5c. PROGRAM ELEMENT NUMBER

6. AUTHOR(S)
Lindsay Hinck

hinck@biology.ucsc.edu

5d. PROJECT NUMBER

5e. TASK NUMBER

5f. WORK UNIT NUMBER

7. PERFORMING ORGANIZATION NAME(S) AND ADDRESS(ES)
University of California, Santa Cruz
MCD Biology
225 Sinsheimer Lab
1156 High Street
Santa Cruz, CA 95064

8. PERFORMING ORGANIZATION REPORT NUMBER

9. SPONSORING / MONITORING AGENCY NAME(S) AND ADDRESS(ES)
U.S. Army Medical Research and Materiel
Fort Detrick, Maryland 21702-5012

10. SPONSOR/MONITOR'S ACRONYM(S)
Command

11. SPONSOR/MONITOR'S REPORT NUMBER(S)

12. DISTRIBUTION / AVAILABILITY STATEMENT

Approved for public release; distribution unlimited

13. SUPPLEMENTARY NOTES

14. ABSTRACT

The research performed over the last twelve months is based on the hypothesis that SLIT/ROBO1 signaling regulates interactions between myoepithelial and luminal epithelial cells, and that loss of this activity results in the destabilization of the basal cell niche. Over the past 12 months, we have extended our analysis on the excess population of stem and progenitor cells discovered in *Slit2-/-;Slit3-/-* and *Robo1-/-* mammary glands. We show that SLIT/ROBO1 signaling restrains the proliferation of basal cells, including stem cells, and that loss of this signaling leads to increased transcription of TCF/LEF targets such as Cyclin-D1. We find that SLIT/ROBO1 signaling regulates the small GTPase Rac, possibly through the Abl tyrosine kinase, and that this regulation may link SLIT/ROBO1 to β-catenin. Our research promises to provide insight into the mechanisms by which normal stem/progenitor cells are regulated, leading to potential insights into how they may be deregulated upon cancerous transformation.

15. SUBJECT TERMS
breast, Slit2, Robo1, basal cell

16. SECURITY CLASSIFICATION OF:			**17. LIMITATION OF ABSTRACT**	**18. NUMBER OF PAGES**	**19a. NAME OF RESPONSIBLE PERSON**
a. REPORT	**b. ABSTRACT**	**c. THIS PAGE**			USAMRMC
U	U	U	UU	16	**19b. TELEPHONE NUMBER** *(include area code)*

Table of Contents

INTRODUCTION:

Myoepithelial cells have recently been termed the "natural tumor suppressor" of the breast because they maintain breast tissue integrity by organizing the cells in contact with them, including cells in the breast stem cell niche, located between the myoepithelial and luminal epithelial cell layers. SLITs are a family of secreted proteins that were originally identified as axon guidance cues in the nervous system. Numerous studies have demonstrated the epigenetic inactivation of *Slits* and *Robos* in multiple types of cancer, including breast, an observation supported by our studies (Marlow et al., 2008). The research we performed over the past 12 months under the auspices of an IDEA Award is based on the hypothesis that SLIT/ROBO1 signaling regulates interactions between myoepithelial and luminal epithelial cells, and that loss of this activity results in the destabilization of the basal cell niche and subsequent formation of ductal lesions with basal characteristics. Over the past 12 months, we have extended our analysis as outlined in last year's report and are in the process of characterizing the stem cells in *Slit2-/-;Slit3-/-* and *Robo1-/-* mammary glands. To perform these studies, we have adopted new techniques (FACS analysis, serial transplantation and mammosphere cultures) that were not described in our funded application but, because the field has moved rapidly, these techniques are now considered standard for stem cell analysis in the mammary gland. We also extended our studies on *Slit2-/-;Slit3-/-* hyperplastic, basal-like lesions and evaluated the effects of the *Slit* loss on surrounding blood vessels. This avenue of investigation was published this year in the *Proceedings of the National Academy of Science* (Marlow et al., 2010).

BODY:

As explained in last year's report, in initiating the work outlined in our funded application, we took the advice of our reviewers' and obtained a histopathological evaluation from Dr. Robert Cardiff who directs the UC Davis Mutant Mouse Pathology Laboratory. Following Dr. Cardiff's suggestion, we serially transplanted *Slit2-/-; Slit3-/-* tissue; we now have multiple lines that demonstrate ~2X longevity (11 generations for *Slit2-/-; Slit3-/-* tissue compared to 6 for +/+ tissue) (Fig. 1). These data, together with other data collected in the past year (see below), suggest that the observed longevity phenotype arises from a stem cell defect, and we have been pursuing this phenotype as explained in last year's report. This does not change the scope of our research, which is focused on understanding the role of SLITs in maintaining the basal cell niche, but it has required adoption of new techniques.

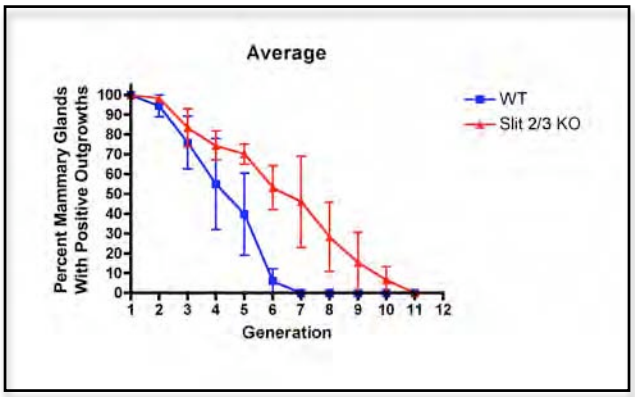

Figure 1: Average longevity of 5 Slit2-/-;Slit3-/- lines compared to +/+. Mammary outgrowths were serially transplanted into pre-cleared Fox^{nu} host fat pads until senescence.

<u>Outline of proposed research for months 12-24 from the Statement of Work:</u>

Aim I: Characterize the hyperplastic lesions observed in Slit2-/-;Slit3-/- and Robo1-/- mammary glands.

PUT in about PNAS

<u>Task 3: Determine the origin of the basal-like cells, (months 12-24).</u>

a. Generate tissue by transplantation.
b. Cross-section occluded ducts and +/+ control ducts in both Slit2/Slit3 KO lines in mature Robo 1 KO glands. Double stain with CK14 to mark basal cells and either nestin (DSHB) or p63 (Abcam). Quantify and document localization in both.

c. Animals required: a) 12 immunocompromised hosts with *Slit2-/-/Slit3-/-* and +/+, and b) 4 *Robo1-/-* females, 3 months of age and +/+ controls.

Aim II: Evaluate whether loss of Slit expression in human breast tumors corresponds with basal tumor characteristics.

Task 4: Survey expression of Slits, Robo and basal markers in human breast tumors, (months 12-24, begins after approval process).

a. Collect frozen samples of normal human breast tissue and tumors.
b. Isolate mRNA and generate cDNA for PCR analysis of expression levels of *Slit2, Slit3* and *Robo1* using specific primers. Use SYBR green with BioRad iCycler Realtime PCR system and analyze results using the Spearman Rank coefficient to correlate expression levels.
c. Confirm protein expression of above genes and basal markers (CK5, CK14, HER1, HER2 and ER alpha) by immunohistochemistry using tissue arrays of matched tumor samples that were used to generate mRNA in part b. All the antibodies identified above for use in mouse tissue also recognize the human protein with the exception of anti-HER1 which will be purchased from Zymed.
d. Human tissue samples required: a-b) 30 tumor samples and 6 reduction mammoplasty control samples will be analyzed. Tissue will be collected in collaboration with Dr. Sukumar after obtaining permission and under the guidelines set forth by the Johns Hopkins Institutional Review Board (JH IRB). c) Tissue array slides supplied by Dr. Sukumar as described above.

Aim III: Identify the signaling effectors in myoepithelial cells that mediate SLIT/ROBO1 adhesion.

Task 6: Demonstrate role for Abl as downstream signaling effector of Slit/Robo1 adhesion, (months 24-36).

a. Dissociate mammary glands with enzymatic digestion from CD1 mice heterozygous for the K14-GFP-actin gene, and isolate the GFP-positive, myoepithelial cell fraction by differential trypsinization. Cells will be transfected with either His-tagged Adeno-Abl or Adeno-Abl-PP and recombined with luminal cells in a 4:1 ratio and placed in rotary culture for 24 hours. Organoids will be harvested, fixed and cryosectioned for analysis of the confocal microscope. Aggregates will be assessed by quantifying the integrity of the myoepithelial outer layer. Infection efficiency will be monitored by immunohistochemistry directed against an epitope tag on Abl constructs.
b. Dissociate mammary glands with enzymatic digestion from *Robo1* -/-; K14-GFP actin +/-mice and isolate the GFP-positive, myoepithelial cell fraction by differential trypsinization. Cells will be transfected with either His-tagged Adeno-Abl or Adeno-Abl-with (T->Y) mutation of phosphorylation sites (Y1114 , Y1587 or Y1073) and recombined with luminal cells in a 4:1 ratio and placed in rotary culture for 24 hours. Aggregates will be analyzed as described above.
c. Animals required: a) 18 CD1 donor animals (6 /set, repeated 3 times), b) 18 *Robo1*-/-,K14-GFPactin donor animals (6/set, repeated 3 times)

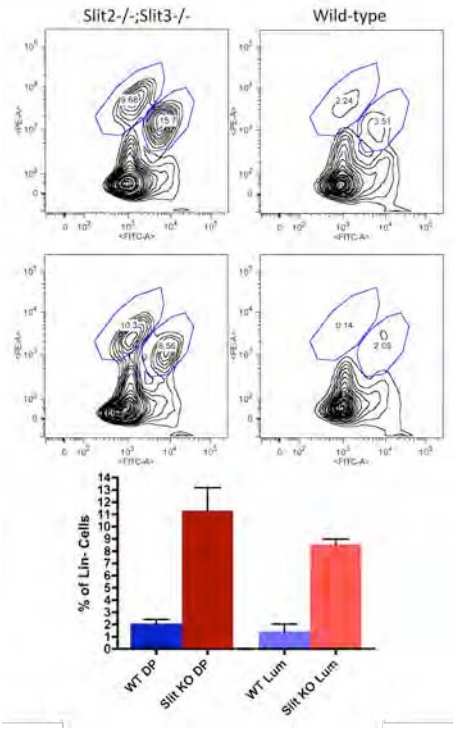

Figure 2: FACS plots and quantification of analysis on generation #4 *Slit2-/-;Slit3-/-* outgrowths compared to wildtype. There are more stem cells (DP: double positive) and luminal progenitors (Lum) in KO compared to +/+ glands.

Results and interpretations:

Aim I: Characterize the hyperplastic lesions observed in Slit2-/-;Slit3-/- and Robo1-/- mammary glands.

Task 3: Determine the origin of the basal-like cells, (months 12-24).

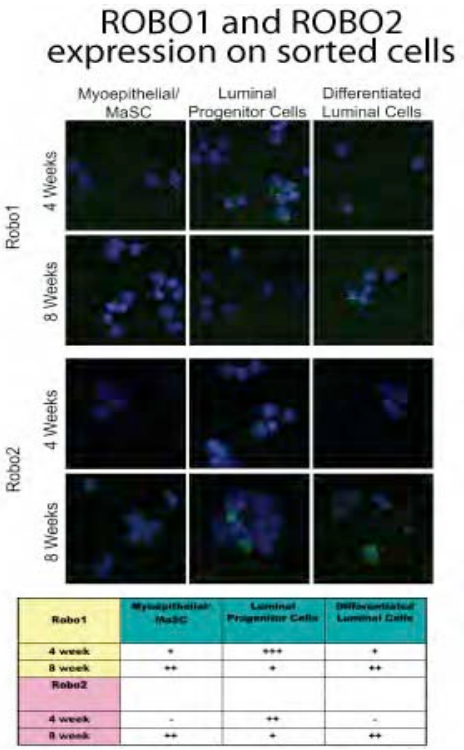

Robo1	Myoepithelial/ MaSC	Luminal Progenitor Cells	Differentiated Luminal Cells
4 week	+	+++	+
8 week	++	+	++
Robo2			
4 week	-	++	-
8 week	++	+	++

Figure 3: Robo receptors are expressed on stem and progenitor as well as mature, differentiated cells. Cytospin preparations of sorted cells immunostained with antibodies directed against ROBO1 and ROBO2.

We have been working hard to characterize the stem cell phenotype in *Slit2-/-;Slit3-/- and Robo1-/-* mammary glands. The use of immuno-markers as we proposed in our funded application (Task 3) has not pinpointed the stem cells as we envisioned. State-of-the-art techniques require FACS sorting, followed by mammosphere or *in vivo* assays (e.g. limiting dilution experiments). Figure 2 shows a FACS sort and quantification of generation 4 *Slit2-/-;Slit3-/-* versus +/+ glands. We find that KO glands contain excess stem cells and luminal progenitors and we are in the process of characterizing these cells by immunohistochemistry on mammospheres. We have had some trouble culturing mammospheres, but recently obtained expert advice from colleagues at the Mammary Gland Gordon conference. Instead of using liquid media for the cultures, we are now embedding the mammospheres in dilute Matrigel and this is giving us healthier looking colonies that we can replate and manipulate. We have also evaluated the profile of ROBO expression in sorted cells and observe both ROBO1 and ROBO2 in stem cells (MaSC) and the luminal progenitor population, suggesting that the effects of SLITs may require signaling through both receptors. We propose to perform serial transplant studies on both receptors to determine whether one or both *Robo* KO lines exhibit the increased longevity observe in the *Slit2-/-;Slit3-/-* lines.

Summary Task 3:

Aim II: Evaluate whether loss of Slit expression in human breast tumors corresponds with basal tumor characteristics.

Task 4: Survey expression of Slits, Robo and basal markers in human breast tumors, (months 12-24, begins after approval process).

Last year, we reported that we did not see significant differences between wild type and *Slit2-/-;Slit3-/-* tissue in the levels of estrogen or progesterone receptor, suggesting that loss of *Slits* and *Robos* will not correspond to basal markers (ER-, PR- Her2-) in human breast tumors. Before using precious human samples for this analysis, we evaluated tumor data on Oncomine and the UCSC Cancer Browser and, again, did not find significant correspondence between *Slit* underexpression and basal markers. Last year, however, we did observe upregulation of Cyclin-D1 and downregulation of E-cadherin in *Slit2-/-;Slit3-/-* outgrowths. Together with our stem cell phenotype, this suggested perturbations in β-catenin signaling since one of the nuclear targets of β-catenin LEF/TCF transcription is Cyclin-D1.

We have pursued this avenue of investigation, focusing initially on *Robo1* because the original hyperplastic phenotype was observed in *Slit2-/-;Slit3-/-* and *Robo1-/-* outgrowths. To investigate, we generated primary myoepithelial (MEC) and primary luminal (LEC) cells from KO versus +/+ outgrowths, treated the cell fractions with SLIT2, and assayed for proliferation by measuring the levels of Cyclin-D1 in each fraction and by measuring the incorporation of EdU. We found that SLIT2 inhibits the proliferation of only myoepithelial cells; luminal cells, that do not express ROBO1, are refractory to the effects of SLIT2 (Fig. 4A). Next, we evaluated cell proliferation *in vivo* in mammary glands. We initially focused on end buds. These are the proliferative structure at the tips of growing ducts that are composed of an outer layer of cap cells that

differentiate into myoepithelial cells, and inner layers of luminal cells. We observed an ~2-fold increase in cap cell proliferation in *Robo1-/-* glands, compared to +/+ (Fig. X), consistent with the cell culture data (Fig. 4B). We also evaluated the consequences of having excess cap cells by examining subtending ducts. In *Robo1-/-* ducts, we observed an overabundance of disorganized myoepithelial cells containing a disrupted actin belt in sections stained with phalloidin, a marker of filamentous actin, whereas wildtype ducts contained a single layer of ordered myoepithelial cells. We also assayed for additional targets of LEF/TCF transcription (Axin2, c-Myc and Tcf1) and found that all of these targets are upregulated in KO compared to +/+ myoepithelial cells. Together, these data suggest that hyperplastic lesions in *Slit2-/-;Slit3-/-* glands have a stem cell phenotype that may be distinct from basal-like. This makes sense in terms of new data on breast tumors. It appears that basal-like tumors may arise from luminal progenitors, whereas stem cells may give rise to heterogenous tumors with many cell types (Lim et al., 2009).

Summary Task 4:

We evaluated whether loss of *Slit* expression in human breast tumors corresponds with basal tumor characteristics in silico, rather than on precious samples, and found no correlation. Instead, it appears that the hyperplastic lesions observed in *Slit2-/-;Slit3-/-* and *Robo1-/-* outgrowths contain excess stem cells due to aberrant β-catenin signaling. This makes sense in terms of recent data suggesting that basal-like cancers arise from luminal progenitors (Lim et al., 2009), whereas stem cells appear to give rise to heterogenous tumors that have both luminal and basal characteristics. Furthermore, as we hypothesized in our funded application, our data support the notion that SLIT/ROBO1 signaling regulates the stem cell niche by regulating β-catenin signaling. Loss of SLIT/ROBO1 signaling results in increases proliferation of the basal cell compartment, leading to increased numbers of stem cells.

Aim III: Identify the signaling effectors in myoepithelial cells that mediate SLIT/ROBO1 adhesion.

Task 6: Demonstrate role for Abl as downstream signaling effector of Slit/Robo1 adhesion, (months 24-36).

The SOW of our funded application calls for us to investigate Abl as a downstream effector of SLIT/ROBO1 adhesion in the coming year (months 24-36). However, this year, we

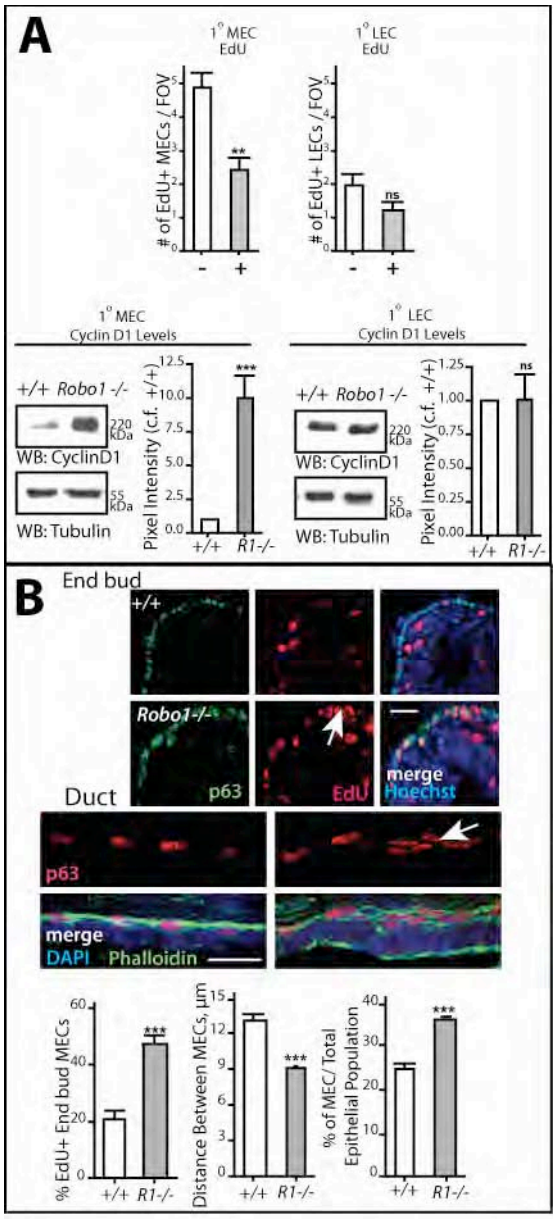

Figure 4: Loss of Robo1 results in excess proliferation of myoepithelial cells.
(A) Quantification of proliferating MECs (CK-14+/EdU+) and LECs (CK-14-/EdU+) (MECs: *n*=3 experiments, >1000 cells per treatment; ***P* <0.001; LECs: *n*=3 experiments, >1000 cells per treatment; ^{ns}P>0.05; *t* test). Increased *Cyclin D1* in *Robo1-/-*, compared to +/+ MECs as assayed by RT-qPCR analysis and Western blot. (MECs: *n*=3 experiments; ***P* <0.001; LECs: *n*=3 experiments; ^{ns}P>0.05; *t* test). (B) Individual channel images of Hoescht stained, EdU-labeled, p63 immunostained +/+ and *Robo1-/-* end buds and ducts. Quantification of cell proliferation as measured by % of EdU+ MEC nuclei, and as distance between MECs in *Robo1-/-*, compared to +/+, ducts (proliferation: *n*=3 animals; ****P* < 0.0001; *t* test). (MEC spacing: *n*=3 animals; ****P* < 0.0001; proportion of MECs to total cells: *n*=3 animals; ****P* < 0.0001; *t* test).

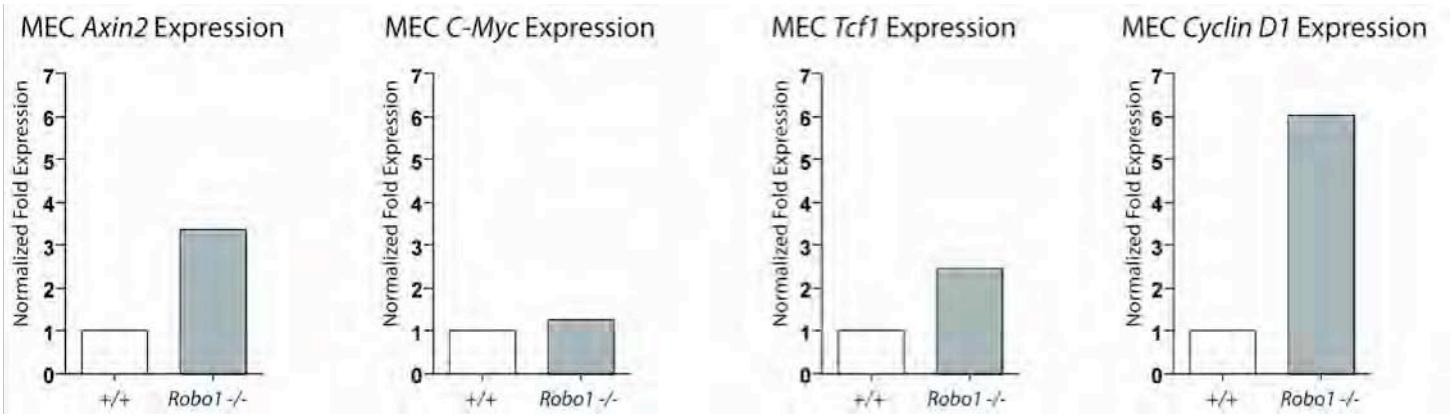

Figure 5: Robo1-/- myoepithelial cells displaly increased expression of b-catenin target genes, Cyclin-D1, Axin2 and Tcf1. RT-qPCR analysis of target gene expression in the myoepithelial cell fraction. (n=1)

noticed in our experiments exploring the stem cell phenotype of *Slit2-/-;Slit3-/-* and *Robo1-/-* outgrowths that the actin belt of myoepithelial cells was greatly disorganized (Fig. 4B, duct, arrow). There is data in the literature showing that Abl functions as a regulatory link between the cadherin–catenin adhesion complex and the actin cytoskeleton through regulation of Rac during adherens junction formation (Zandy et al., 2007). This was intriguing to us given our data presented in Figures 1-5 showing regulation of β-catenin transcriptional activity by SLIT/ROBO1 signaling. β-catenin is a central cellular regulator, functioning as both a transcriptional regulator and an adhesive protein complexed with cadherin. Because this phenotype was present in our KO outgrowths and it presented a link to Abl, we initiated studies to examine the role of Rac as a downstream effector of Slit/Robo1.

Thus far, we have documented that SLIT2 activates Rac and that this activation remodels the actin cytoskeleton. Figure 6 shows pull-down assays on lysates from primary cultures of mammary cells using a GST fusion protein of the PAK1 binding domain (GST-PBD) that binds activated Rac1. A comparison of wildtype and knockout cells reveals an approximately 66% decrease in activated Rac1 in *Robo1-/-* animals. Conversely, when we assessed the effects of adding recombinant SLIT2 to wildtype cells, we observed an approximately 2.5-fold increase in Rac1 activity. To determine whether the increase in Rac1 activity occurs in myoepithelial cells that express ROBO1, we purified them, added recombinant SLIT2 and performed pull-down assays. Again, we observed a significant increase in Rac1 activity in response to SLIT2 treatment.

As we propose to do in our Abl experiments (Task 6, SOW), we have also used viruses to explore the consequences of Rac1 activation in myoepithelial cells. For these experiments, we used HME50 cells, an immortalized myoepithelial cells line. We infected HME50 cells with constitutively active Rac1 (Ad-Rac1 L61-Flag) and observed an abundance of stress fibers in positive cells as assayed by staining with phalloidin. To confirm that these effects could be attributed to SLIT/ROBO1 signaling, we treated HME50 cells with SLIT2 and again stained with phalloidin. SLIT2 treatment recreated the increase in stress fibers observed with constitutively active Rac1. Stress fibers were not induced with SLIT treatment if cells were pretreated with a Rac1 inhibitor (NSC23766), suggesting that Rac1 activation is required for SLIT2-mediated stress fiber formation.

<u>Summary Task 6:</u>

We identified Rac and actin as downstream effectors of SLIT/ROBO1 adhesion. Abl regulates Rac during adherens junction formation to mediate interactions between the cadherin–catenin adhesion complex and

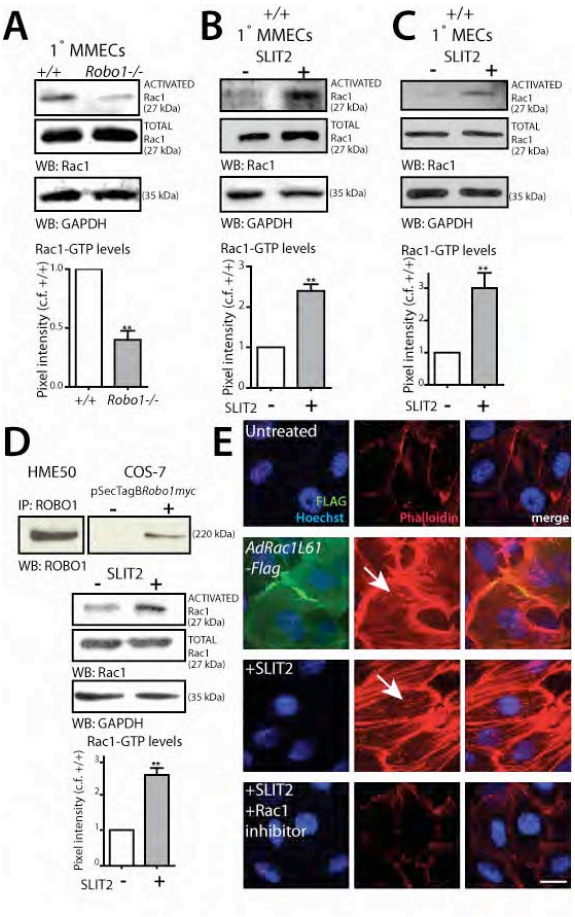

Figure 6: Slit/Robo1 signaling activate Rac to organize the actin cytoskeleton. (A-C) Primary MMECs, either total myoepithelial and luminal epithelial cells (A, B) or myoepithelial-enriched cultures (C) were lysed and assayed for activated Rac1 using p21-activated kinase binding domain (PAK1-PBD). (A) Decreased levels of activated Rac1 in the absence of *Robo1* and, conversely, (B, C) increased levels upon SLIT2 treatment *Top*: representative immunoblots for GTP-Rac1, total Rac1, and loading control GAPDH. *Bottom*: quantitative analysis of Rac1 activation. (*n*=3 experiments; ** *P*<0.001; *t* test). (D) ROBO1 expression in human MEC cell line HME50 as revealed by immunoprecipitation/immunoblotting of HME50 and control COS-7 cells transfected with pSecTagB*Robo1myc*. HME50 lysates display increased actived Rac1 levels after SLIT2 treatment (*n*=3 experiments; ** *P*<0.001; *t* test.) (E) Similar morphological changes in cells infected with activated Rac1 (Rac1-N19-Flag) or treated with SLIT2. Individual channel images showing FLAG staining to detect activated Rac1 (green), phalloidin (red) and DAPI nuclei (blue). Merged images reveal increased stress fibers in HME50 cells either infected with activated Rac1 or treated with SLIT2. Scale bars: 10μm (E).

the actin cytoskeleton. Here we show that SLIT/ROBO1 is also upstream of Rac and the effects we observe on the actin cytoskeleton may be through the Abl pathway. Thus, we are delineating a pathway (SLIT/ROBO1/Abl/Rac/b-catenin) that may control the proliferation and adhesion of basal cells (including stem cells) in the gland. Our future studies, as outlined in the SOW, will focus on how Abl function downstream of Slit/Robo.

Recommended changes in future work to better address the research topic:

- Transplant studies on both receptors to determine whether one or both *Robo* KO lines exhibit the increased longevity observe in the *Slit2-/-;Slit3-/-* lines

KEY RESEARCH ACCOMPLISHMENTS:

- Identified a stem cell signature in *Slit2-/-;Slit3-/-* glands
- Showed that loss of SLIT/ROBO1 signaling disrupts basal cell proliferation by interfering with β-catenin signaling
- Discovered Rac as a downstream effector of SLIT/ROBO1 signaling and potential link to Abl signaling in the gland.
- Published paper in *PNAS* identifying the effects of losing *Slit* expression in epithelium on mammary vasculature

REPORTABLE OUTCOMES:

Paper:

Marlow R., Binnewies M., Sorensen L.K., Monica S. D., Strickland P., Forsberg E.C., Li D.Y., Hinck L. 2010. Vascular Robo4 Restricts Pro-Angiogenic VEGF Signaling in Breast, *Proc Natl Acad Sci U S A*. Jun 8;107(23):10520-5. PMID: 20498081

Abstracts:

Gwyn Harburg and Lindsay Hinck. The Role of SLIT/ROBO Signaling in Mammary Stem Cell Self-Renewal and Progenitor Cell Fate. *Mammary Gland Biology Gordon Conference*. June 6-11, 2010.

CONCLUSIONS:

Evidence is growing that myoepithelial cells function as "natural tumor suppressors" because they organize tissue structure, including cells in the breast stem cell niche, and generate the barrier between epithelium and stroma by secreting the basal lamina. Over the second year of this IDEA Award, my laboratory has continued our characterization of the basal-like, hyperplastic lesions that occur in mammary glands harboring loss-of-function mutations in *Slit2* and *Slit3*. This characterization led to the unanticipated discovery of effects of *Slit* loss on the surrounding vasculature. We pursued this observation and published a paper describing these effects this year in PNAS. The rest of our data are presented in this annual report.

We evaluated by immunohistochemical analysis as outlined in our SOW and by *in silico* analysis the hypothesis proposed in our funded application that basal-like *Slit2-/-;Slit3-/-* lesions fit the triple-negative profile. However, we did not observe significant differences between *Slit2-/-;Slit3-/-* and +/+ tissue using triple negative markers and *in silico* analysis did not reveal a correlation between *Slit* loss and basal-like breast tumors. As outlined in last year's annual report, we proceeded to pursue the characterization of a stem-cell like phenotype in *Slit2-/-;Slit3-/-* glands. Our new data suggest that, instead of having a triple-negative profile, *Slit2-/-;Slit3-/-* tumors have a stem cell phenotype, characterized by misregulation of the β-catenin signaling pathway leading to excess proliferation of a population of stem/progenitor cells. We have begun to characterize this signaling pathway and our initial studies support the notion that SLIT/ROBO1 signaling regulates the Abl tyrosine kinase which, in turn, regulates Rac to regulate β–catenin. Other pathways (e.g. PI-3 kinase/Akt signaling) may be in involved as well (Prasad et al., 2008), but our studies are delineating a novel pathway by which SLIT/ROBO1 signaling modulates mammary basal cell adhesion and cell proliferation by regulating β-catenin.

In sum, the stem cell hypothesis for breast tumors posits that cancer stem cells, a small population of self-renewing cells within a tumor, are responsible for breast cancer progression and recurrence. This suggests that the targets of malignant transformation are normal stem/progenitor cells. Many laboratories are attempting to identify and characterize cancer stem cells. These efforts will be greatly aided by a better understanding of normal stem cells: their identification *in situ* and elucidation of their regulation during normal development. Our data suggest that SLITs regulate at least one population of stem cells. Our continued research to characterize the *Slit2-/-;Slit3-/-* longevity phenotype under the auspices of the DoD promises to provide insight into the mechanisms by which normal stem/progenitor cells are regulated, leading to potential insights into how they may be deregulated upon cancerous transformation.

REFERENCES:

Lim, E., Vaillant, F., Wu, D., Forrest, N. C., Pal, B., Hart, A. H., Asselin-Labat, M. L., Gyorki, D. E., Ward, T., Partanen, A. et al. (2009). Aberrant luminal progenitors as the candidate target population for basal tumor development in BRCA1 mutation carriers. *Nat Med* **15**, 907-13.

Marlow, R., Strickland, P., Lee, J. S., Wu, X., Pebenito, M., Binnewies, M., Le, E. K., Moran, A., Macias, H., Cardiff, R. D. et al. (2008). SLITs suppress tumor growth in vivo by silencing Sdf1/Cxcr4 within breast epithelium. *Cancer Res* **68**, 7819-27.

Prasad, A., Paruchuri, V., Preet, A., Latif, F. and Ganju, R. K. (2008). Slit-2 induces a tumor-suppressive effect by regulating beta-catenin in breast cancer cells. *J Biol Chem* **283**, 26624-33.

Zandy, N. L., Playford, M. and Pendergast, A. M. (2007). Abl tyrosine kinases regulate cell-cell adhesion through Rho GTPases. *Proc Natl Acad Sci U S A* **104**, 17686-91.

APPENDICES:

- pdf of our paper in *PNAS*

SUPPORTING DATA: Figures are embedded in the text.

Vascular Robo4 restricts proangiogenic VEGF signaling in breast

Rebecca Marlow[a], Mikhail Binnewies[a], Lise K. Sorensen[b], Stefanie D. Monica[a], Phyllis Strickland[a], E. Camilla Forsberg[c], Dean Y. Li[b], and Lindsay Hinck[a,1]

[a]Department of Molecular, Cell and Developmental Biology, University of California, Santa Cruz, CA 95064; [b]Department of Oncological Sciences, University of Utah, Salt Lake City, UT 84112; and [c]Department of BioMolecular Engineering, University of California, Santa Cruz, CA 95064

Edited* by Gail Martin, University of California, San Francisco, CA, and approved April 28, 2010 (received for review February 16, 2010)

Formation of the vascular system within organs requires the balanced action of numerous positive and negative factors secreted by stromal and epithelial cells. Here, we used a genetic approach to determine the role of SLITs in regulating the growth and organization of blood vessels in the mammary gland. We demonstrate that vascularization of the gland is not affected by loss of *Slit* expression in the epithelial compartment. Instead, we identify a stromal source of SLIT, mural cells encircling blood vessels, and show that loss of *Slit* in the stroma leads to elevated blood vessel density and complexity. We examine candidate SLIT receptors, *Robo1* and *Robo4*, and find that increased vessel angiogenesis is phenocopied by loss of endothelial-specific *Robo4*, as long as it is combined with the presence of an angiogenic stimulus such as preneoplasia or pregnancy. In contrast, loss of *Robo1* does not affect blood vessel growth. The enhanced growth of blood vessels in *Robo4*$^{-/-}$ endothelium is due to activation of vascular endothelial growth factor (VEGF)-R2 signaling through the Src and FAK kinases. Thus, our studies present a genetic dissection of SLIT/ROBO signaling during organ development. We identify a stromal, rather than epithelial, source of SLITs that inhibits blood vessel growth by signaling through endothelial ROBO4 to down-regulate VEGF/VEGFR2 signaling.

angiogenesis | ROBO | SLIT | mammary gland | organogenesis

Recent studies on the SLIT family of axon guidance molecules have demonstrated a conserved role in regulating development of the vascular system. However, a comprehensive understanding of their vascular function has been hampered by contradictory findings (1). SLITs have been shown to both attract (2–6) and repel (7–9) endothelial cells. ROBO1, which binds directly to SLITs, has been shown to promote endothelial cell motility, either alone (2, 6, 10) or as a heterodimeric partner with ROBO4 (5, 9). In contrast, ROBO4 binds SLITs at either very low affinity or not at all and likely requires a coreceptor, such as ROBO1 or a Syndecan, to signal (5, 11, 12). ROBO4 has been assigned the repellent functions of SLITs (7, 8) and, more recently, an alternative role in countering the effects of vascular endothelial growth factor (VEGF) to provide vascular stabilization (13, 14). One experimental variable that may be responsible for these contradictory findings is that many studies were performed in vitro using recombinant SLIT protein prepared in a variety of ways (2, 5, 6, 8, 13, 15). Here, we circumvent the requirement for recombinant protein by taking a genetic approach to address the function of SLIT in a biological context using the mammary gland as a model system. Such an approach provides insight into the role of endogenous SLIT/ROBO signaling in mammary development and angiogenesis.

During postnatal mammary gland development, the epithelium elaborates a bilayered, tree-like structure as it grows from the nipple subdermally through the surrounding stromal environment (16). The stroma is composed of adipocytes, fibroblasts, immune cells and a limited number of principal arteries supplying the capillary plexuses that envelop ducts. The gland undergoes stereotyped cycles of cell growth and differentiation under the influence of estrus and pregnancy hormones. In the virgin, the estrus cycle does not cause expansion of the vasculature, but pregnancy is accompanied by robust capillary sprouting that provides increased blood supply to promote lobulo-alveolar expansion (17, 18). Classic studies on vascular patterning of the gland demonstrated the importance of the epithelium because its absence resulted in only the major vessels and none of the duct-associated capillary plexuses (17). One explanation for this observation is that the epithelium acts as an important source of vascular endothelial growth factor (VEGF) (19–22) and possibly other factors, such as guidance cues. VEGF is also up-regulated in breast tumors, stimulating angiogenesis and fueling cancer cell growth (23). Thus, epithelial VEGF plays an important role in regulating angiogenesis in the mammary gland. In contrast, little is known about the role of guidance cues such as SLITs in directing blood vessel growth and organization during organ development.

We previously demonstrated the expression of SLITs in mammary gland epithelium (24). Here, we identify a second source of SLIT, mural cells associated with blood vessels. We use transplantation experiments to determine the compartment, epithelial or stromal, in which SLIT/ROBO signaling occurs. We show that stromal, but not epithelial, SLITs inhibit vessel growth by down-regulating VEGFR signaling through ROBO4; ROBO1 is not required for this inhibition. However, loss of the inhibitory action of SLIT, alone, does not stimulate vessel growth. This requires additional positive factors such as SDF1 or VEGF, and we demonstrate that preneoplasia or pregnancy supplies these proangiogenic molecules. Together, these studies elucidate a role for SLIT/ROBO signaling in maintaining vascular homeostasis during mammary morphogenesis.

Results

Loss of Global, but Not Epithelial, *Slit* Expression Leads to Increased Blood Vessel Number and Complexity. To determine SLIT function during mammary gland development, we initially focused on epithelial SLITs as a target-derived source because previous studies have reported directional migration of endothelial cells in response to exogenous or tumor-supplied SLIT protein (2, 4, 7, 8). Only *Slit2* and *Slit3* are expressed by mammary epithelia (24); therefore, to evaluate the consequences of losing epithelial SLIT expression, we generated *Slit2*$^{-/-}$;*Slit3*$^{-/-}$ chimeric mammary outgrowths by transplantation because the *Slit2*$^{-/-}$ mutation is perinatal lethal (Fig. 1*A*) (25). This technique involved placing small fragments of adult epithelium into contralateral fat

Author contributions: R.M., M.B., P.S., and L.H. designed research; R.M., M.B., L.K.S., S.D.M., and P.S. performed research; E.C.F. and D.Y.L. contributed new reagents/analytic tools; R.M., M.B., L.K.S, S.D.M., P.S., E.C.F, D.Y.L, and L.H. analyzed data; and R.M. and L.H. wrote the paper.

Conflict of interest statement: D.Y.L. is employed by the University of Utah, which has filed intellectual property surrounding the therapeutic uses of targeting Robo4 and with the intent to license this body of intellectual property for commercialization.

*This Direct Submission article had a prearranged editor.

[1]To whom correspondence should be addressed. E-mail: hinck@biology.ucsc.edu.

This article contains supporting information online at www.pnas.org/lookup/suppl/doi:10.1073/pnas.1001896107/-/DCSupplemental.

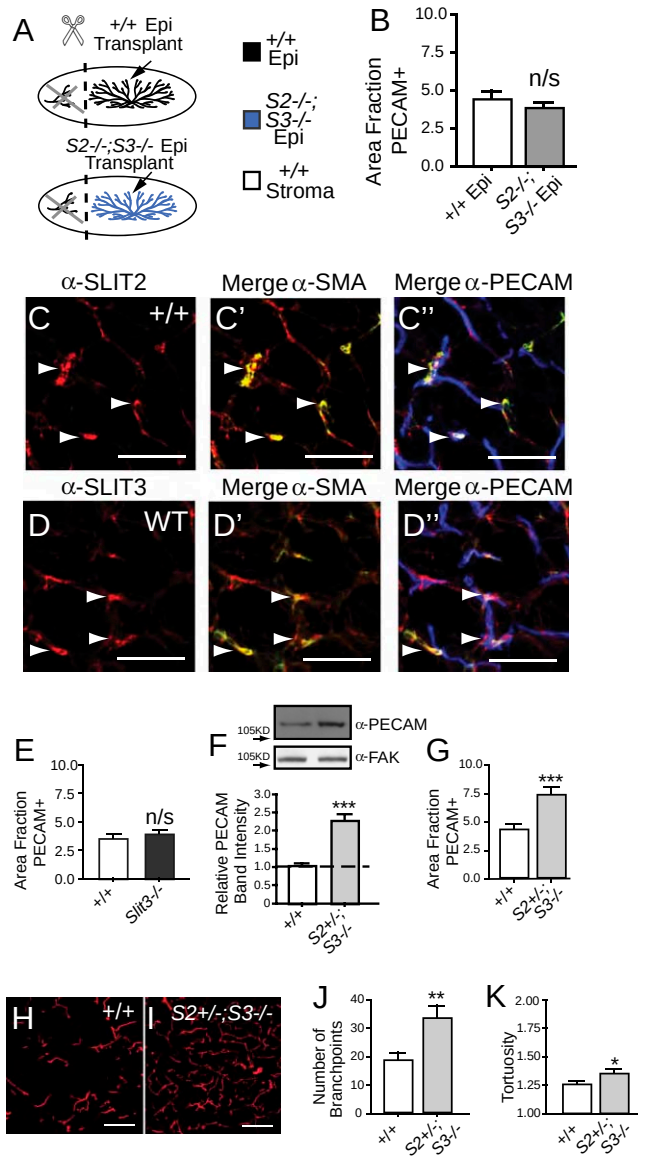

Fig. 1. Loss of global, but not epithelial *Slits*, enhances blood vessel growth. (*A*) Diagram illustrating transplants that generate chimeric mammary glands with *Slit2*$^{-/-}$;*Slit3*$^{-/-}$ epithelium (blue) and contralateral WT epithelium (black), transplanted into immunocompromised (*Foxn1*^{nu}) hosts (white) that have been precleared of their WT epithelium (black). (*B*) Lack of *Slit* in the epithelium does not alter blood vessel density in outgrowths. Quantitative analysis of PECAM-positive pixel area (n = 3 contralateral outgrowths, 15 fields of view (FOV)/outgrowth). Error bars = SEM. n/s = not significant. (*C* and *D*) Mural cells express SLIT2 and SLIT3. Representative images of sections immunostained for PECAM (blue), SMA (green), and SLIT2 or SLIT3 (red). Arrows indicate mural cell localization. (Scale bar, 50 μm.) (*E*) Lack of *Slit3* does not increase blood vessel number in the mammary gland. Quantitative analysis of PECAM-positive pixel area (n = 3 animals, 15 FOV/gland). Error bars = SEM. n/s = not significant. (*F–K*) Global lack of *Slit* significantly increases blood vessel number and network complexity. (*F*) Representative PECAM immunoblots on WT and *Slit2*$^{+/-}$;*Slit3*$^{-/-}$ mammary lysates (50 μg loaded; FAK immunoblot is loading control). Bar graph represent quantitative analysis of PECAM band intensity (ImageJ) (n = 3). Error bars = SEM, ***$P < 0.001$ unpaired t test. (*G*) Quantitative analysis of PECAM-positive pixel area (n = 3 animals, 15 FOV/animal). Error bars = SEM. *** $P < 0.001$ unpaired t test. (*H* and *I*) Representative images of WT (*H*) and *Slit2*$^{+/-}$;*Slit3*$^{-/-}$ (*I*) mammary sections immunostained with anti-PECAM (red). (Scale bar = 50 μm.) (*J*) Number of branchpoints and (*K*) tortuosity of blood vessels were quantified. Error bars = SEM, ***$P < 0.001$, **$P < 0.005$, *$P < 0.01$ unpaired t test.

pads of immunocompromised (*Foxn1*$^{nu-/-}$) host mice that have been precleared to remove endogenous epithelium (26). After 10 weeks, the fragments have grown into mature epithelial trees and the entire gland was harvested. Blood vessel density was analyzed by immunostaining for blood vessel marker PECAM and quantified. We observed no significant difference in blood vessel density between transplants containing WT or *Slit2*$^{-/-}$;*Slit3*$^{-/-}$ epithelium (Fig. 1*B* and Fig. S1 *A* and *B*), suggesting that endothelial cells are refractory to the loss of epithelial SLIT.

It has been reported that *Slit2* and *Slit3* are expressed in cells surrounding the vasculature (6, 13), suggesting the presence of a stromal source for SLITs, at least in some tissues. We performed immunohistochemistry on sections of adult mammary gland with antibodies directed against SLIT2 or SLIT3, PECAM, and the mural cell marker, SMA. We observe strong colocalization of SMA with both SLITs, demonstrating expression of SLIT in support cells surrounding blood vessels. We also observe weaker colocalization of SLITs with PECAM that may reflect cell-associated SLIT, either secreted from surrounding support cells or a consequence of low level SLIT expression by endothelial cells (Fig. 1 *C* and *D* and Fig. S1 *C* and *D*). These studies identify a stromal source of SLITs that may exert a local effect on vessel growth and organization.

To evaluate the consequences of knocking out *Slit3* in both the epithelia and stroma, we examined intact, adult glands of mice that were homozygous null for *Slit3* and observed no changes in blood vessel density (Fig. 1*E* and Fig. S1 *E* and *F*). This suggests that, unlike the embryonic diaphragm (6), SLIT3 functions redundantly with SLIT2 in the adult mammary gland. To evaluate the consequences of depleting both *Slits*, we examined intact glands of mice that are homozygous for *Slit3* and heterozygous for *Slit2* because the *Slit2* null mutation is lethal (*Slit2*$^{+/-}$; *Slit3*$^{-/-}$). In these glands, we observe an approximately two-fold increase in blood vessel density and a significant increase in the complexity of the vessel network (Fig. 1 *F–K*). This analysis shows that a single functional allele of *Slit2* is insufficient to supply the SLIT required to restrict blood vessel growth in the mammary gland. Together with the absence of phenotype in transplanted *Slit2*$^{-/-}$;*Slit3*$^{-/-}$ glands in which *Slits* are knocked out in the epithelium alone (Fig. 1*B*), the data suggest that stromal SLITs function at short-range to restrain the growth of mammary gland endothelial cells.

Combined Loss of *Robo1* and *Robo4* Leads to Increased Vessel Density. To evaluate the roles of ROBO1 and ROBO4 in mammary gland vasculature, we examined their loss-of-function phenotypes because phenocopy of *Slit2*$^{+/-}$;*Slit3*$^{-/-}$ defects provides strong genetic evidence that one, or both, of these receptors functions in the same pathway. ROBO4 has been identified as an endothelial specific mediator of SLIT signaling and its removal is not lethal to the animal (13, 14). To evaluate its loss-of-function phenotype, we analyzed intact, adult *Robo4*$^{-/-}$ and WT glands and did not observe a significant difference in the number of blood vessels (Fig. 2*A* and Fig. S2 *A* and *B*).

Next, we examined the expression of ROBO1 in blood vessels because it is unclear whether it is expressed by all types of endothelial cells (2, 7). We performed immunohistochemical analysis on WT glands using anti-ROBO1 (27) and found it colocalized in a membrane-associated pattern with PECAM (Fig. 2*B*). We confirmed these results by taking advantage of the expression of LacZ in knockout tissue under the control of the endogenous *Robo1* promoter and found positive staining in *Robo1*$^{-/-}$ blood vessels (Fig. S2 *C* and *D*). Thus, in our system, ROBO1 is expressed on blood vessels and may serve as a SLIT receptor. To investigate, we evaluated the loss-of-function phenotype in intact, adult *Robo1*$^{-/-}$ and WT glands and did not observe a significant difference in blood vessel number (Fig. 2*C*).

Because analysis of the single knock-out *Robo1* and *Robo4* glands did not yield a phenotype, we generated and analyzed

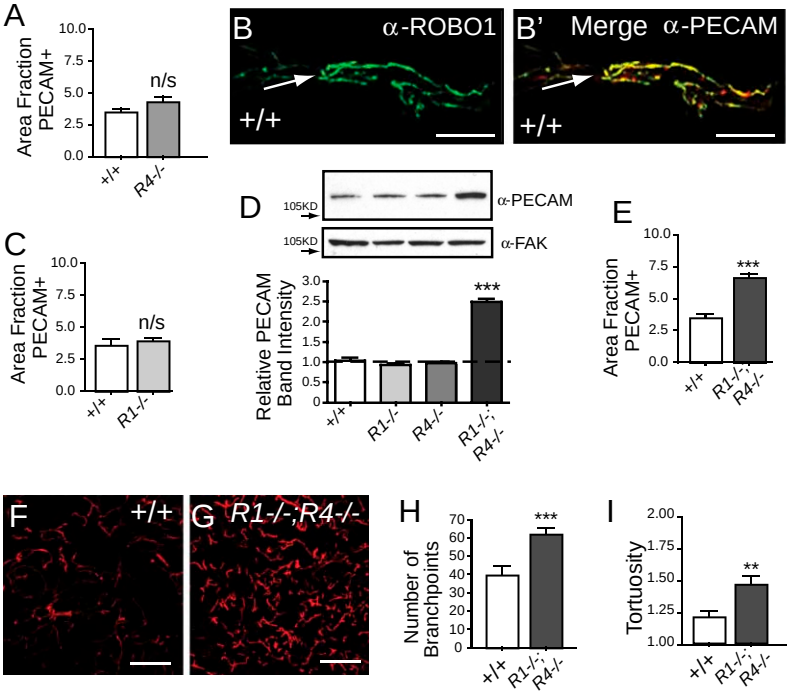

Fig. 2. Loss of ROBO1 and ROBO4 enhances blood vessel growth. (*A*) Lack of *Robo4* does not alter blood vessel density in the mammary gland. Quantitative analysis of PECAM-positive pixel area ($n = 3$ animals, 15 FOV/animal). Error bars = SEM. n/s = not significant. (*B*) ROBO1 is expressed by blood vessels. Representative images of ROBO1 (green) and PECAM (red) immunostaining on WT mammary sections. (Scale bar, 20 μm.) (*C*) Lack of *Robo1* does not alter blood vessel density in the mammary gland. Quantitative analysis of PECAM-positive pixel area ($n = 3$ animals, 15 FOV/animal). Error bars = SEM. n/s = not significant. (*D–I*) Lack of both *Robo1* and *Robo4* significantly increases blood vessel density and network complexity in the mammary gland. (*D*) Representative PECAM immunoblots on WT, Robo1$^{-/-}$, Robo4$^{-/-}$, and *Robo1*$^{-/-}$;*Robo4*$^{-/-}$ mammary lysates (50 μg loaded; FAK immunoblot is loading control). Bar graph represent quantitative analysis of PECAM band intensity (ImageJ) ($n = 3$). Error bars = SEM, ***$P < 0.001$ ANOVA. (*E*) Quantitative analysis of PECAM-positive pixel area ($n = 4$ animals, 15 FOV/animal). ***$P < 0.001$ unpaired *t* test. (*F* and *G*) Representative images of WT (*F*) and *Robo1*$^{-/-}$;*Robo4*$^{-/-}$ (*G*) mammary sections immunostained with anti-PECAM (red). (Scale bar, 50 μm.) (*H* and *I*) Quantification of branchpoint number (*H*) and tortuosity (*I*). Error bars = SEM. ***$P < 0.001$, **$P < 0.005$ unpaired *t* test.

Robo1$^{-/-}$;*Robo4*$^{-/-}$ mice. We discovered an approximately twofold increase in blood vessel density and complexity in *Robo1*$^{-/-}$;*Robo4*$^{-/-}$ glands (Fig. 2 *D–I* and Fig. S2 *E* and *F*) that was similar to the increase observed in *Slit2*$^{+/-}$;*Slit3*$^{-/-}$ glands (Fig. 1 *F–K*). These results demonstrate that loss of both SLIT receptors is required to achieve increased blood vessel density.

***Robo4*$^{-/-}$ Blood Vessels Display Enhanced Angiogenesis in Response to SDF1 and VEGF.** Our studies show that generating a blood vessel surplus, similar to that observed in *Slit2*$^{+/-}$;*Slit3*$^{-/-}$ glands, requires loss of both *Robo1* and *Robo4*. One explanation for this requirement is that each receptor compensates for the other in restraining vessel growth and only loss of both ROBO receptors leads to increased density. Alternatively, there may be an epithelial effect because these analyses were performed on intact, rather than transplanted, glands. ROBO1 is expressed in the epithelium (24), as well as the endothelium (Fig. 2*B* and Fig S2 *C* and *D*), raising the possibility that loss of *Robo1* in the epithelium contributes to the observed increase in blood vessel density in the *Robo1*$^{-/-}$;*Robo4*$^{-/-}$ mice. Indeed, we previously showed that epithelial loss of *Robo1* generates disorganized, hyperplastic tissue that is characterized by up-regulation of the chemokine CXCL12, also known as stromal derived factor-1 (SDF1) (27).

SDF1 induces the expression of VEGF in breast cancer cell lines (28) and normal breast epithelium (Fig. S3*A*). Therefore, we evaluated the expression of SDF1 and VEGF in *Robo1*$^{-/-}$ tissue and found that loss of *Robo1*, either alone or in combination with *Robo4*, resulted in up-regulation of both SDF1 and VEGF-A in mammary epithelium (Fig. 3 *A* and *B* and Fig. S3 *B–J*). To determine whether the angiogenic phenotype in *Robo1*$^{-/-}$;*Robo4*$^{-/-}$ glands is attributable to the loss of *Robo1* in the epithelium and consequent up-regulation of proangiogenic factors, we generated chimeric mammary glands by transplantation. First, we transplanted *Robo1*$^{-/-}$ and WT epithelial fragments into WT fat pads (Fig. 3*C*). After 10 weeks of outgrowth, we examined the number and complexity of blood vessels and observed no difference between the outgrowths (Fig. 3*D* and Fig S3 *K* and *L*), suggesting that loss of epithelial *Robo1*, alone, is insufficient to increase blood vessel density.

Next, we examined the angiogenic phenotype in glands that combined loss of epithelial *Robo1* with loss of stromal *Robo4*. We generated these chimeric glands by transplanting *Robo1*$^{-/-}$ and contralateral WT epithelium into *Robo4*$^{-/-}$ fat pads and examined the number and complexity of blood vessels after 10 weeks of outgrowth (Fig. 3*E*). We found a significant increase in blood vessel density in glands containing *Robo1*$^{-/-}$ epithelium combined with *Robo4*$^{-/-}$ stroma (Fig. 3 *F–H* and Fig S3 *M* and *N*), similar to the increase observed in *Robo1*$^{-/-}$;*Robo4*$^{-/-}$ (Fig. 2 *D–I*) and *Slit2*$^{+/-}$;*Slit3*$^{-/-}$ glands (Fig. 1 *F–K*). Together, these data show that the presence of ROBO1 in the endothelium does not compensate for the loss of ROBO4. Instead, ROBO4 appears to function alone in the endothelium as an angiogenesis inhibitor. To examine whether there are other contexts in which ROBO4 mediates SLIT signaling in the absence of ROBO1, we performed migration assays on Human Lung MicroVascular Endothelial Cells-Lung (HMVEC-L) (Fig. 3*I*). These cells express low levels of *Robo1* and robust levels of *Robo4*, both of which could be selectively knocked down using siRNAs. We observed that VEGF stimulated migration of these cells was reduced by the N-terminal fragment of SLIT2, a reduction that occurred upon knockdown of *Robo1*, but not *Robo4*, providing another example where ROBO4 transduces a SLIT signal, even when *Robo1* expression is greatly diminished or absent.

Together, our studies suggest that ROBO1 contributes to the *Robo1*$^{-/-}$;*Robo4*$^{-/-}$angiogenic phenotype through its role in the epithelium as a negative regulator of SDF1 and VEGF-A (Fig. 3 *A* and *B* and Fig. S3 *B–J*). The up-regulation of proangiogenic cues that occurs in *Robo1*$^{-/-}$ mammary epithelium generates a pre-pathological environment. However, this alone was insufficient to increase angiogenesis because we found that, in addition, loss of *Robo4* was also necessary (Figs. 2 *D–I* and 3 *D–I*). This process of pathological angiogenesis in response to proangiogenic cues has previously been documented in the visual system of *Robo4*$^{-/-}$ animals (13). However, it is unknown whether the loss of *Robo4*, alone, will result in increased angiogenesis during normal developmental processes, in part because there are few examples of robust blood vessel growth in the adult animal. In the mammary gland, however, there is a normal developmental event, pregnancy, associated with exuberant sprouting angiogenesis (18) that is driven by VEGF-A

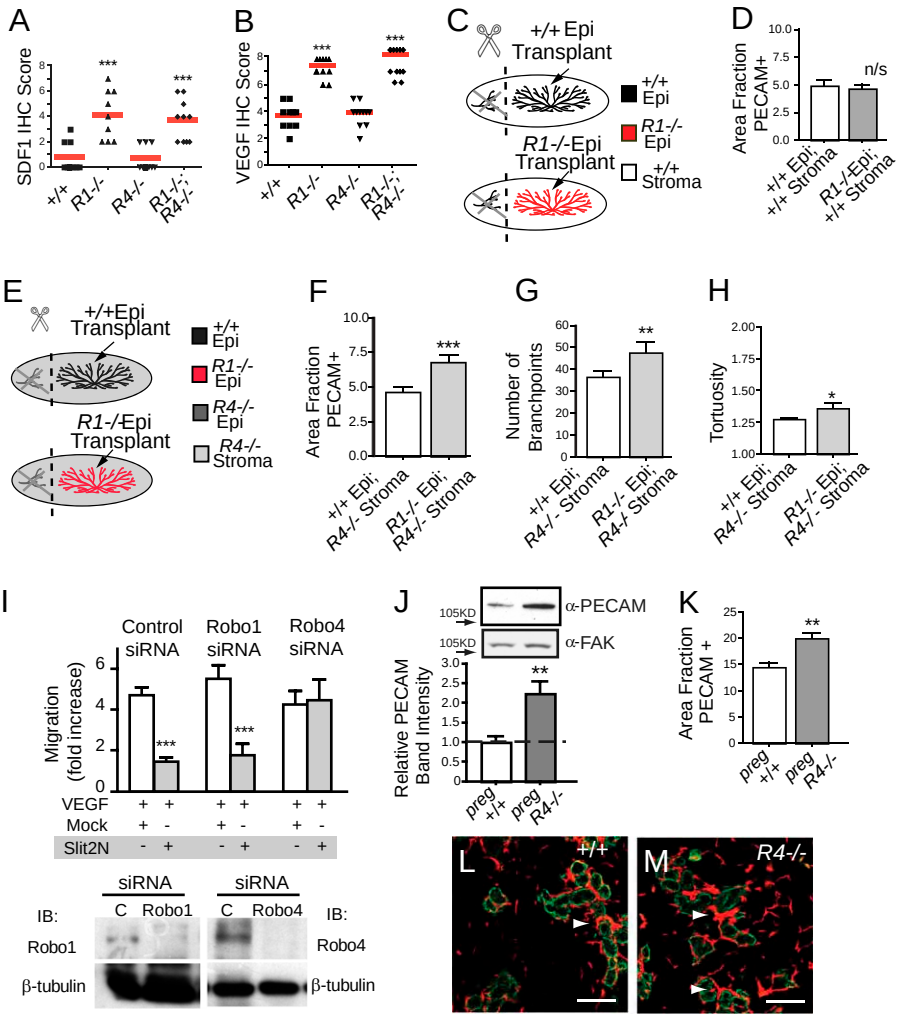

Fig. 3. The proangiogenic factor, VEGF, emanating from *Robo1*$^{-/-}$ and pregnant epithelium increases angiogenesis in *Robo4*$^{-/-}$ glands. (*A* and *B*) SDF1 (*A*) and VEGF-A (*B*) are expressed at higher levels by *Robo1*$^{-/-}$ and *Robo1*$^{-/-}$;*Robo4*$^{-/-}$, compared to WT or *Robo4*$^{-/-}$, mammary glands. Immunostained sections were scored according to cell percent positivity and staining intensity ($n = 3$ animals, 10 FOV/animal). Scores were plotted on a vertical scatter plot and red bars indicate average score. ***$P < 0.001$ ANOVA. (*C*) Diagram illustrating generation of chimeric glands with *Robo1*$^{-/-}$ epithelium (red) and contralateral WT epithelium (black), transplanted into immunocompromised (*Foxn1*^{nu}) hosts (white) that have been cleared of their WT epithelium (black) (*D*) Lack of *Robo1* in the epithelium does not alter blood vessel density in outgrowths. Quantification of PECAM-positive pixel area [$n = 7$ contralateral outgrowths, 15 FOV/outgrowth]. Error bars = SEM. n/s = not significant. (*E*) Diagram illustrating generation of chimeric glands with *Robo1*$^{-/-}$ epithelium (red) and contralateral WT epithelium (black) into syngeneic *Robo4*$^{-/-}$ background (light gray) that have been cleared of their host *Robo4*$^{-/-}$ epithelium (dark gray). (*F–H*) Increased blood vessel density with loss of *Robo1* in the epithelium combined with the loss of *Robo4*. (*F*) Quantitative analysis of PECAM-positive pixel area ($n = 3$ contralateral outgrowths, 15 FOV/outgrowth). Quantification of branchpoint number (*G*) and tortuosity (*H*). Error bars = SEM, **$P < 0.005$, *$P < 0.01$ unpaired *t* test. (*I*) *Robo4* is necessary for SLIT2N-mediated inhibition of VEGF-induced human microvascular endothelial cells-lung (HMVEC-L) migration. HMVEC-L cells were subjected to control, *Robo1*, or *Robo4* siRNA and allowed to migrate in response to VEGF in the presence of Mock or SLIT2N ($n > 3$, *** $P < 0.001$ ANOVA). Western blot analysis confirmed knockdown of *Robo1* or *Robo4* expression. (*J–M*) Pregnancy increases blood vessel density in *Robo4-/-* glands compared to WT. (*J*) Representative immunoblots of anti-PECAM on WT and *Robo4*$^{-/-}$mammary lysates (50 μg loaded; FAK immunoblot is loading control). Bar graph represents quantification of PECAM band intensity (ImageJ) ($n = 3$). Error bars = SEM, ***$P < 0.001$ unpaired *t* test. (*K*) Quantitative analysis of PECAM-positive pixel area ($n = 3$ animals, 10 FOV/animal). Error bars = SEM, **$P < 0.005$ unpaired *t* test. (*L* and *M*) Representative images of WT (*L*) and *Robo4*$^{-/-}$ (*M*) mammary sections from animals at pregnancy day 12.5 immunostained with anti-PECAM (red) and anti-CK14 (green), a marker for myoepithelial cells. Arrowheads indicate capillary baskets surrounding alveoli. (Scale bar, 50 μm.)

(19, 20) (Fig. S3*O*). To evaluate the consequences of *Robo4* loss in this context, we analyzed midpregnant *Robo4*$^{-/-}$ glands and found a significant increase in blood vessel density (Fig. 3*J–M*). These data show that a normal developmental event, pregnancy, results in excessive sprouting angiogenesis in the absence of *Robo4*.

ROBO4 Restrains VEGF/VEGFR Signaling. One model proposed for SLIT/ROBO4 signaling is that it functions to restrain pathologic angiogenesis by inhibiting VEGF/VEGFR2 signaling (13). We examined the activation of VEGFR2 by evaluating its autophosphorylation status in *Robo4*$^{-/-}$ glands under two proangiogenic conditions: hyperplasia, due to loss of *Robo1*$^{-/-}$, and pregnancy. We observed an approximately twofold increase in phosphorylation in extracts from *Robo1*$^{-/-}$;*Robo4*$^{-/-}$ glands, compared to WT, *Robo1*$^{-/-}$, or *Robo4*$^{-/-}$ gland extracts (Fig. 4*A*). Moreover, a similar increase in VEGFR2 activation was observed in extracts from pregnant *Robo4*$^{-/-}$, compared to pregnant WT, glands (Fig. 4*B*). We confirmed this increase in VEGFR2 signaling by immunohistochemistry using anti-PY1175 VEGFR2 (Fig. 4*C* and Fig. S4 *A–D*). Next, we examined whether this increase in VEGFR phosphorylation activated downstream signaling pathways by immunoblotting for phospho-Src (PY416) (Fig. 4*D*) and immunostaining for phospho-FAK (PY-397) (Fig. 4*E* and Fig. S4 *E–H*). We

found up-regulated VEGFR2 signaling in hyperplastic *Robo1*$^{-/-}$;*Robo4*$^{-/-}$ and pregnant *Robo4*$^{-/-}$ glands. Altogether the data show that loss of *Robo4* under conditions that favor angiogenesis, tissue hyperplasia or pregnancy, leads to increased VEGF/VEGFR2 signaling (Fig. 4) and increased angiogenesis (Figs. 2 *D–I* and 3 *F–H*, *L*, and *M*).

Discussion

Here, we took advantage of a relatively simple, but highly manipulable, model system of organ development to examine the role of SLIT guidance cues in regulating vascular development during postnatal mammogenesis. This involves the elaboration of an extensive vascular bed and the generation of ductal capillary plexuses, concomitant with expansive growth of the epithelial mammary tree (18). There have been many conflicting reports describing the response of cultured endothelial cells to SLIT, but few studies examining the role of SLIT/ROBO signaling in regulating angiogenesis and vascular remodeling in vivo (6, 13). Our data show that blood vessels respond to a stromal source of SLIT that signals through a ROBO4-mediated pathway to counter VEGF/VEGFR signaling and restrain angiogenesis (Fig. S5). In contrast, ROBO1 on endothelial cells does not appear to restrain vessel growth. Taken together, our studies support a recently proposed model for SLIT/ROBO4 function based on studies of pathologic angiogenesis in the retina (13). Both in this context and in the mammary gland, there are two requirements for increased angiogenesis (1): elimination of the restraining function of ROBO4 and (2) provision of a proangiogenic cue such as VEGF (Figs. 2 *D–G*, 3 *F–H* and *J–M*, 4, and Fig S5).

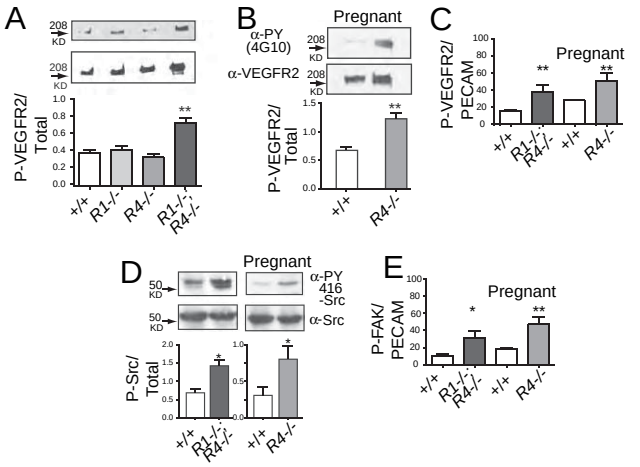

Fig. 4. ROBO4 functions to restrain VEGF/VEGFR2 signaling in the mammary gland. (*A*) Increased activation of VEGFR2 in *Robo1*$^{-/-}$;*Robo4*$^{-/-}$ but not WT, *Robo1*$^{-/-}$ or *Robo4*$^{-/-}$ glands. Immunoblotting for VEGFR2 and phosphotyrosine (4G10) after immunoprecipitation of VEGFR2 from adult gland lysates. Bar graph represents quantification of phospho-VEGFR2 relative to total VEGFR2 (ImageJ) ($n = 4$ per stage and per genotype). Error bars = SEM, $^{**}P < 0.005$ unpaired *t* test. (*B*) Increased activation of VEGFR2 in *Robo4*$^{-/-}$ in pregnant glands (day 12.5) compared to WT. Bar graph represents quantification of phospho-VEGFR2 relative to total VEGFR2 (ImageJ) ($n = 3$). Error bars = SEM, $^{**}P < 0.005$ unpaired *t* test. (*C*) Increased activation of VEGFR2 in *Robo1*$^{-/-}$;*Robo4*$^{-/-}$ adult glands and *Robo4*$^{-/-}$ pregnant glands, compared to WT controls. Bar graphs represent area fraction of pixels positive for PY1175-VEGFR2 divided by the area fraction positive for PECAM ($n = 4$ animals/genotype, 10 FOV/animal). Error bars = SEM, $^{**}P < 0.005$ ANOVA. (*D*) Increased activation of Src in *Robo1*$^{-/-}$;*Robo4*$^{-/-}$ adult virgin glands and *Robo4*$^{-/-}$ pregnant (day 12.5) glands, compared to WT controls. Representative immunoblots for Src and P-Y416-Src on mammary lysates (50 μg loaded). Bar graph represent quantitative analysis of Src and P-Y416-Src band intensity (ImageJ) ($n = 3$). Error bars = SEM, $^{*}P < 0.01$ unpaired *t* test. (*E*) Increased activation of FAK in *Robo1*$^{-/-}$;*Robo4*$^{-/-}$ adult virgin glands and *Robo4*$^{-/-}$ pregnant (day 12.5) glands compared to WT controls. Bar graphs represent the area fraction of pixels positive for PY397-FAK divided by the area fraction positive for PECAM ($n = 4$ animals, 10 FOV/animal). Error bars = SEM, $^{*}P < 0.01$, $^{**}P < 0.005$ ANOVA.

The identity of the SLIT receptor on blood vessels is unclear because both ROBO1 and ROBO4 have been implicated in endothelial cell migration (2, 7, 10, 29). Surprisingly, we found in mammary gland that loss of neither *Robo4* nor *Robo1*, alone, affected blood vessel growth but, instead, the absence of both ROBO receptors was required to generate the increased angiogenesis observed in *Slit2*$^{+/-}$;*Slit3*$^{-/-}$ glands. This was perplexing because the current model for SLIT/ROBO signaling in endothelium proposes the formation of a heterodimeric complex of receptors, with ROBO1 responsible for SLIT binding and ROBO4 functioning in signal transduction (5). If this heterodimeric complex were present on mammary blood vessels, then we would expect loss of either *Robo1* or *Robo4* to yield a phenotype, because both would be required to transduce the SLIT signal.

One of the authors (D.Y.L.) and coworkers, however, recently showed using the retina as an in vivo model system that loss of *Robo4*, alone, yielded a phenotype in the adult animal during the process of pathological angiogenesis (13). In this study, no phenotype was found in *Robo4*$^{-/-}$ animals during development that occurred normally with no apparent defects in vasculogenesis or angiogenesis. When evaluating the mammary gland phenotypes generated by loss of both *Robo1* and *Robo4*, we realized that loss of either *Slit* or *Robo1* in our mammary model system causes a secondary, potentially proangiogenic effect: up-regulation of SDF1 and VEGF (Fig. 3 *A* and *B* and Fig. S3 *A–J*) (27). There is growing evidence that SDF1 and VEGF collaborate to stimulate neoangiogenesis occurring in response to tumors, wounds, and chronic inflammatory disorders (28, 30, 31). Together, these factors contribute to the rapid proliferation of blood vessels observed during pathological angiogenesis. Our data show that up-regulation of these proangiogenic cues, due to loss of *Slit* or *Robo1*, functions as a "stimulatory cue" in our model system (Fig. 3 *A*, *B*, *F–H*, *J–M* and Fig. S3). Absent of this effect, ROBO1 does not appear to play a significant role transducing the inhibitory SLIT signal in blood vessels as evidenced by (*i*) the lack of phenotype in *Robo1*$^{-/-}$ glands (Figs. 2*C* and 3*D* and Figs. S2 *E* and *F* and S3 *K* and *L*), and (*ii*) the increase in vessel density in chimeric glands containing *Robo1*$^{-/-}$ epithelium and *Robo4*$^{-/-}$ endothelium (Fig. 3 *F–H* and Fig. S3 *M* and *N*).

Our data show a clear genetic interaction between SLITs and ROBO4. Moreover, there is recently published evidence that SLITs activate a ROBO4-initiated downstream signaling cascade (6, 14). However, it is still unclear whether SLITs bind directly to ROBO4. Direct interactions have been demonstrated by coimmunoprecipitation assays (6, 7), but the interaction cannot be duplicated with recombinant protein in Biacore assays (15). Thus, it seems likely that a coreceptor is required to transmit SLIT binding into ROBO4 activation. In some contexts, ROBO1 may fulfill this function (5), whereas in other contexts it may be served by receptors such as a Syndecan (11, 12).

Datasets from microarray analyses on human breast tumor samples show decreased *Robo4* expression in human breast cancer (32), colorectal cancer (33), and prostate tumors (34). Our study suggests one explanation for this finding. Environments that require growth, such as tumor microenvironments, may down-regulate *Robo4* expression to enhance the blood supply to cancerous cells because SLIT/ROBO4 signaling inhibits VEGF-mediated angiogenesis. These studies suggest that one way a proangiogenic tumor environment reduces SLIT/ROBO4 signaling and releases the brake on VEGF/VEGFR signaling is by downregulating *Robo4* expression.

The recent model proposed for ROBO4 action, in which it counters the activation of VEGF/VEGFR signaling, limited its role to pathological processes in the retina. Here, we present evidence that ROBO4 also restrains blood vessel growth during

the nonpathological expansion of epithelium and endothelium occurring in mammary gland in preparation for milk production and delivery. VEGF-A is the prime candidate for mediating this rapid increase in capillary number achieved by sprouting angiogenesis (19, 20, 35), but an unanswered question is how its actions are regulated during this short burst of pregnancy-associated angiogenesis that is coupled with rapid epithelial expansion. This period of development must be tightly regulated to prevent loss of growth control that would contribute to tumor development (36). We find that loss of *Robo4* during mid-pregnancy, when VEGF-A expression is at its highest (19), leads to a significant increase in the vascular density of the gland (Fig. 3 *J–M*). This corresponds to increased VEGFR2 autophosphorylation and activation of downstream signaling pathways (Fig. 4). Thus, down-regulation or silencing of *Robo4* expression during pregnancy or involution, periods of active tissue remodeling, could contribute to a tumor microenvironment and may play a role in the transient increase in breast cancer risk observed following pregnancy (37). Taken together, our results indicate a guardianship role for *Robo4* in normal development, when we propose it functions to restrain VEGF/VEGFR2 signaling during sprouting angiogenesis that generates alveolar blood supply.

In conclusion, the findings presented in this report identify the importance of locally-derived SLIT in restraining vascular growth during pregnancy and early stages of breast transformation. This study comprehensively addresses the contribution of both SLIT and their ROBO receptors to vascular development during mammalian organogenesis. Our data support a role for this signaling axis in inhibiting endothelial cell proliferation by downregulating the activation of downstream Src and FAK family kinases and, consequently, counteracting VEGF-VEGFR signaling.

Materials and Methods

Animals. All mice were harvested as adults (10- to 12-wk-old). The study conformed to guidelines set by the Institutional Animal Care and Use Committee (IACUC) at the University of California, Santa Cruz. *Slit2*, *Slit3*, *Robo1*, and *Robo4* null mice were generated as described (13, 24). Transplant techniques, antibodies, immunohistochemistry, migration assays, RT-PCR, immunoprecipitation, immunoblotting, image processing, statistical analyses and determination of blood vessel density, branchpoints and tortuosity are described in detail in *SI Materials and Methods*.

ACKNOWLEDGMENTS. We thank Hector Macias and Jennifer Compton for critical reading of the manuscript and Jennifer Compton and Angel Moran for genotyping. *Slit3*$^{-/-}$ mice were generously provided by Dr. Ornitz (Washington University, St. Louis, MO) and *Slit2*$^{-/-}$ and *Robo1*$^{-/-}$ mice by Dr. Tessier-Lavigne (Genentech Inc., South San Francisco, CA). This research was funded by the National Institutes of Health (RO1 CA-128902), Congressionally Directed Medical Research Program (W81XWH-08-1-0380), and Santa Cruz Cancer Benefit Group.

1. Klagsbrun M, Eichmann A (2005) A role for axon guidance receptors and ligands in blood vessel development and tumor angiogenesis. *Cytokine Growth Factor Rev* 16: 535–548.
2. Wang B, et al. (2003) Induction of tumor angiogenesis by Slit-Robo signaling and inhibition of cancer growth by blocking Robo activity. *Cancer Cell* 4:19–29.
3. Kaur S, et al. (2006) Robo4 signaling in endothelial cells implies attraction guidance mechanisms. *J Biol Chem* 281:11347–11356.
4. Howitt JA, Clout NJ, Hohenester E (2004) Binding site for Robo receptors revealed by dissection of the leucine-rich repeat region of Slit. *EMBO J* 23:4406–4412.
5. Sheldon H, et al. (2009) Active involvement of Robo1 and Robo4 in filopodia formation and endothelial cell motility mediated via WASP and other actin nucleation-promoting factors. *FASEB J* 23:513–522.
6. Zhang B, et al. (2009) *Repulsive Axon Guidance Molecule Slit3 Is a Novel Angiogenic Factor.* Blood 114:4300–4309.
7. Park KW, et al. (2003) Robo4 is a vascular-specific receptor that inhibits endothelial migration. *Dev Biol* 261:251–267.
8. Seth P, et al. (2005) Magic roundabout, a tumor endothelial marker: Expression and signaling. *Biochem Biophys Res Commun* 332:533–541.
9. Kaur S, et al. (2008) Silencing of directional migration in roundabout4 knockdown endothelial cells. *BMC Cell Biol* 9:61.
10. Wang LJ, et al. (2008) Targeting Slit-Roundabout signaling inhibits tumor angiogenesis in chemical-induced squamous cell carcinogenesis. *Cancer Sci* 99: 510–517.
11. Hu H (2001) Cell-surface heparan sulfate is involved in the repulsive guidance activities of Slit2 protein. *Nat Neurosci* 4:695–701.
12. Steigemann P, Molitor A, Fellert S, Jäckle H, Vorbrüggen G (2004) Heparan sulfate proteoglycan syndecan promotes axonal and myotube guidance by slit/robo signaling. *Curr Biol* 14:225–230.
13. Jones CA, et al. (2008) Robo4 stabilizes the vascular network by inhibiting pathologic angiogenesis and endothelial hyperpermeability. *Nat Med* 14:448–453.
14. Jones CA, et al. (2009) Slit2-Robo4 signalling promotes vascular stability by blocking Arf6 activity. *Nat Cell Biol* 11:1325–1331.
15. Suchting S, Heal P, Tahtis K, Stewart LM, Bicknell R (2005) Soluble Robo4 receptor inhibits in vivo angiogenesis and endothelial cell migration. *FASEB J* 19:121–123.
16. Hinck L, Silberstein GB (2005) Key stages in mammary gland development: The mammary end bud as a motile organ. *Breast Cancer Res* 7:245–251.
17. Soemarwoto IN, Bern HA (1958) The effect of hormones on the vascular pattern of the mouse mammary gland. *Am J Anat* 103:403–435.
18. Djonov V, Andres AC, Ziemiecki A (2001) Vascular remodelling during the normal and malignant life cycle of the mammary gland. *Microsc Res Tech* 52:182–189.
19. Pepper MS, et al. (2000) Regulation of VEGF and VEGF receptor expression in the rodent mammary gland during pregnancy, lactation, and involution. *Dev Dyn* 218: 507–524.
20. Hovey RC, Goldhar AS, Baffi J, Vonderhaar BK (2001) Transcriptional regulation of vascular endothelial growth factor expression in epithelial and stromal cells during mouse mammary gland development. *Mol Endocrinol* 15:819–831.
21. Rossiter H, et al. (2007) Inactivation of VEGF in mammary gland epithelium severely compromises mammary gland development and function. *FASEB J* 21:3994–4004.
22. Qiu Y, et al. (2008) Mammary alveolar development during lactation is inhibited by the endogenous antiangiogenic growth factor isoform, VEGF165b. *FASEB J* 22: 1104–1112.
23. Fox SB, Generali DG, Harris AL (2007) Breast tumour angiogenesis. *Breast Cancer Res* 9:216.
24. Strickland P, Shin GC, Plump A, Tessier-Lavigne M, Hinck L (2006) Slit2 and netrin 1 act synergistically as adhesive cues to generate tubular bi-layers during ductal morphogenesis. *Development* 133:823–832.
25. Plump AS, et al. (2002) Slit1 and Slit2 cooperate to prevent premature midline crossing of retinal axons in the mouse visual system. *Neuron* 33:219–232.
26. Robinson GW, Accili D, Hennighausen L (2000) *Rescue of Mammary Epithelium of Early Lethal Phenotypes by Embryonic Mammary Gland Transplantation as Exemplified with Insulin Receptor Null Mice* (Kluwer Academic/Plenum Press, New York), pp 307–316.
27. Marlow R, et al. (2008) SLITs suppress tumor growth in vivo by silencing Sdf1/Cxcr4 within breast epithelium. *Cancer Res* 68:7819–7827.
28. Liang Z, et al. (2007) CXCR4/CXCL12 axis promotes VEGF-mediated tumor angiogenesis through Akt signaling pathway. *Biochem Biophys Res Commun* 359: 716–722.
29. Huminiecki L, Gorn M, Suchting S, Poulsom R, Bicknell R (2002) Magic roundabout is a new member of the roundabout receptor family that is endothelial specific and expressed at sites of active angiogenesis. *Genomics* 79:547–552.
30. Grunewald M, et al. (2006) VEGF-induced adult neovascularization: Recruitment, retention, and role of accessory cells. *Cell* 124:175–189.
31. Lima e Silva R, et al. (2007) The SDF-1/CXCR4 ligand/receptor pair is an important contributor to several types of ocular neovascularization. *FASEB J* 21:3219–3230.
32. Richardson AL, et al. (2006) X chromosomal abnormalities in basal-like human breast cancer. *Cancer Cell* 9:121–132.
33. Gröne J, et al. (2006) Robo1/Robo4: Differential expression of angiogenic markers in colorectal cancer. *Oncol Rep* 15:1437–1443.
34. Latil A, et al. (2003) Quantification of expression of netrins, slits and their receptors in human prostate tumors. *Int J Cancer* 103:306–315.
35. Goldhar AS, Vonderhaar BK, Trott JF, Hovey RC (2005) Prolactin-induced expression of vascular endothelial growth factor via Egr-1. *Mol Cell Endocrinol* 232:9–19.
36. McDaniel SM, et al. (2006) Remodeling of the mammary microenvironment after lactation promotes breast tumor cell metastasis. *Am J Pathol* 168:608–620.
37. Schedin P (2006) Pregnancy-associated breast cancer and metastasis. *Nat Rev Cancer* 6:281–291.